Rovibrationally inelastic scattering of (v=1, j=1) H-2 from Cu(100) experiment and theory

Watts, E.; Sitz, G.O.; McCormack, D.A.; Kroes, G.; Olsen, R.A.; Groeneveld, J.; van Stralen, J.N.P.; Baerends, E.J.; Mowrey, R.C.

State-to-state scattering in a reactive system: H$_2$(v=1,J=1) from Cu(100)

Elizabeth Watts and Greg O. Sitz[a)]

Department of Physics, University of Texas, Austin, Texas 78712

We have measured state-to-state scattering in the H$_2$–Cu(100) and H$_2$–Cu(110) systems for H$_2$ initially prepared in the $v=1,J=1$ state, for several final (v,J) states. We observe survival in the initial state ($v=1,J=1$), rotational excitation within $v=1$ (into $v=1,J=3$), and rotational excitation plus vibrational relaxation into final states ($v=0,J=5$) and ($v=0,J=7$). For each of these final states, we measure the branching fraction (relative to the incident $v=1,J=1$ flux) and the mean final translational energy. In addition, for rotational excitation from $J=1$ to 3, the dependence on initial translational energy and surface temperature is measured within $v=1$ and compared with results within $v=0$. Our results are compared with published state-resolved associative desorption results, similar scattering experiments, and recent theoretical calculations. © *2001 American Institute of Physics.* [DOI: 10.1063/1.1344233]

I. INTRODUCTION

The H$_2$–copper system has been a testing ground for chemical dynamics at surfaces for over 25 years,[1,2] in part because it is a simple system in which dissociation is activated. In spite of the large amount of work that has been done, this situation shows no signs of changing. The definitive experiments to date have been energy- and state-resolved measurements of the product H$_2$ following recombinative (or associative) desorption.[1] These experiments, plus earlier beam studies of dissociative adsorption,[3] have revealed the presence of a substantial (roughly 0.6 eV) energy barrier to dissociation as well as a number of interesting dynamical effects involving internal, molecular degrees of freedom.

The H$_2$–copper system has also been the subject of intense theoretical study,[2,4–6] primarily because of its electronic simplicity. The first step is the calculation (or empirical construction) of a potential-energy surface (PES) for the molecule–surface system. In the past five years, a number of such surfaces have been computed for H$_2$–metal systems, notably copper,[7] and palladium.[8,9] These surfaces are commonly thought to be accurate to within roughly 0.1 eV.

Starting with the PES, dynamics calculations are performed to compute dissociation probabilities for molecules incident from the gas phase as a function of energy and quantum state.[6] The principle of detailed balance is used to relate these probabilities to the experimentally measured desorption populations. Alternatively, theoretical results are convolved over experimental conditions to compare with molecular beam adsorption data. Clearly, in this later situation, greater specificity in preparing the molecules in the incident beam provides for a more stringent comparison with calculations.

Final state distributions for molecules which do not dissociate are also obtained in these calculations, but not as much attention has been devoted to these results in the past, since the corresponding experiments were not common. Recently, however, such experiments have matured, and there now exists the opportunity for direct comparison between experiment and theory at an advanced level. Two recent model calculations that deal with inelastic scattering focused on the aspects of the final state distributions resulting from the reactive character of the PES. Miura *et al.* studied rotational and vibrational state effects in the H$_2$–Cu(111) system.[10] They found rotational excitation increased faster with increasing incident translational energy for vibrationally excited molecules. They explained this in terms of a greater decrease in vibrational energy near the transition state to dissociation for $v=1$ molecules than for $v=0$. The vibrational energy that was freed up could appear in rotation. Wang, Darling, and Holloway also investigated rotational transitions in the H$_2$–Cu(111) system.[11] They presented a model in which the effective potential acts on a molecule with an extended bond. The bond extension happens as the molecule starts to explore the ''elbow'' region of the PES. The extended bond results in a compression of the manifold of rotational states making transitions among them easier. This idea is similar to what we have suggested to explain the surface temperature dependence of rotational excitation in the H$_2$–Pd(111) system,[12,13] and which we will revisit for the H$_2$–copper system in this paper.

The calculated PES's for the dissociation of a diatomic molecule typically show strong variation of the energy with essentially all molecular degrees-of-freedom (DOF).[4,7] Because of this, strong couplings between the internal molecular DOFs during scattering from a reactive surface are predicted. Based on this, we expect that studies of inelastic scattering in a reactive system should provide a stringent test of current understanding of molecule surface dynamics. This

---

[a)]Electronic mail: gositz@physics.utexas.edu

is part of the motivation for the present study. A detailed comparison between experiment and theory will be presented elsewhere;[14] here we focus on a complete presentation of the experimental results.

The state-to-state scattering approach has been applied recently in both the H_2–copper[15–18] and H_2–palladium[19] systems. Hodgson et al.[16] reported several novel features in the scattering of $H_2(v=1,J)$ from Cu(111). For $H_2(v=1,J=0)$ they found a sharp threshold for rotational excitation (from $J=0$ to $J=2$) with increasing incident translational energy followed by a plateau at energies above about 140 meV. They also found a dramatic decrease in reflected $v=1$ signal for energies above about 150 meV. They interpreted this as evidence for vibrational relaxation, although they were not able to directly observe this process. They were also unable to observe rotational excitation for $H_2(v=1,J=1)$ and placed a lower limit for the probability of less than a few percent. On Pd(111) Gostein et al.[19] observed vibrational relaxation of $H_2(v=1,J=1)$ into $(v=0,J=5)$ and $(v=0,J=7)$. By measuring the final translational energy for these states, they were able to show that a significant amount of the energy released in the vibrational relaxation is lost to surface degrees-of-freedom. Rettner et al.[15] observed vibrational excitation for H_2 scattered from Cu(111). Although their experiment was not fully state-to-state, they found that the rotational distribution was cooler in the excited vibrational state ($v=1$) than in the incident ($v=0$) distribution. Based on a theoretical study of this process, McCormack et al.[20] concluded that the observed rotational cooling arose because rotational energy was used to furnish part of the energy for vibrational excitation.

As mentioned above, dissociation of H_2 on copper surfaces is activated, with a barrier of roughly 0.6 eV.[21] Vibrational excitation is thought to be less effective than an equivalent amount of energy in translation on overcoming this barrier.[22] However, since the quantum of vibrational energy in H_2 is roughly 0.5 eV, we expect that this excitation plus translational energies in the range of 0.1–0.3 eV, should allow incident molecules to sample regions of the PES in the vicinity of the dissociation barrier.

Here we report fully state-to-state scattering measurements for H_2 prepared in the $(v=1,J=1)$ state for a range of incident translational energies and surface temperatures. We discuss our findings in relation to state- and energy-resolved desorption results[1] and also with respect to recent calculations of elastic, inelastic and dissociative scattering for the $H_2(v=1)$–Cu(100) system.[2,5]

II. EXPERIMENT

The experimental setup has been described in detail previously[17–19] and will only be summarized here. The apparatus consists of a doubly differentially pumped molecular beam source coupled to an ultrahigh vacuum (UHV) scattering chamber. The source is a pulsed nozzle that produces a supersonic beam of H_2 at a repetition rate of 10 Hz. The translational energy of the molecules is varied by heating or cooling the nozzle; temperatures range from 200 to 900 K, resulting in H_2 translational energies from 35 meV to 200

meV. The gas pulse passes first through a skimmer into a buffer chamber. The buffer chamber contains a chopper rotating at 300 Hz; this produces pulses of roughly 6 μs duration. The beam passes through a second aperture and impinges on a single crystal Cu(100) surface at near-normal incidence.

The Cu surface is cleaned approximately every three hours according to standard procedures.[12] The surface is maintained at a temperature between 100 and 800 K during a scattering experiment by means of an electron beam heater mounted behind the sample holder and coupling to a liquid nitrogen cooled copper block. Most experiments were done at a surface temperature of 500 K; given that the sticking coefficient for H_2 is so low under our conditions, the surface remains free of adsorbed H. During the course of the experiment the sample is flashed above 875 K every thirty minutes to remove any CO or H_2O which may have built up.

State preparation in the incident beam is accomplished using stimulated Raman scattering (SRS). The incident molecular beam pulse is crossed at a right angle with two, focused laser beams. The frequency difference of the two lasers matches the $Q(1)$ line of the H_2 vibrational Raman band, and efficiently excites molecules from the ground vibrational state to the first excited vibrational state. One of these colors (the pump light) is the second harmonic of a Nd:YAG laser at 532 nm. The second color (the Stokes light) is generated by simulated Raman scattering of the first in a cell pressurized with 5 atm of H_2. One advantage of this approach is that the Stokes light is automatically offset by the right amount from the pump, since the H_2 molecule itself determines the frequency shift. A second advantage is that the pump and Stokes beams emerging from the high pressure cell are co-linear, making optical alignment easier.

The probe laser beam is focused into the molecular beam 0.4–2.5 mm in front of the surface where it state-selectively ionizes the molecules through a (2+1) resonance enhanced multiphoton ionization (REMPI) process.[23] These ions are collected and then detected with a microchannel electron multiplier plate. The probe light used is the third harmonic of a tunable Nd:YAG pumped dye laser. By varying the firing time of the probe laser relative to that of the nozzle, a time-of-flight (TOF) profile of the incident gas pulse is obtained. The pump laser is set to fire at the peak of the incident distribution. By varying the time delay of the probe laser relative to the pump laser, a second type of the TOF spectrum is obtained showing molecules resulting from the Raman excitation step (incident, scattered or both; examples are shown in Figs. 1, 2, and 7 and discussed below). The probe beam can be accurately translated in the direction of propagation of the molecular beam: by recording TOF spectra at a series of focal positions the incident and scattered translational energies can be determined. This technique is essential, since small sample displacements affect the TOF peak positions. For example, the sample holder thermally expands by about 0.0005 inches when the sample temperature is changed by 500 K, and this is readily observed in the scattered TOF spectra. Different ro-vibrational states are ob-
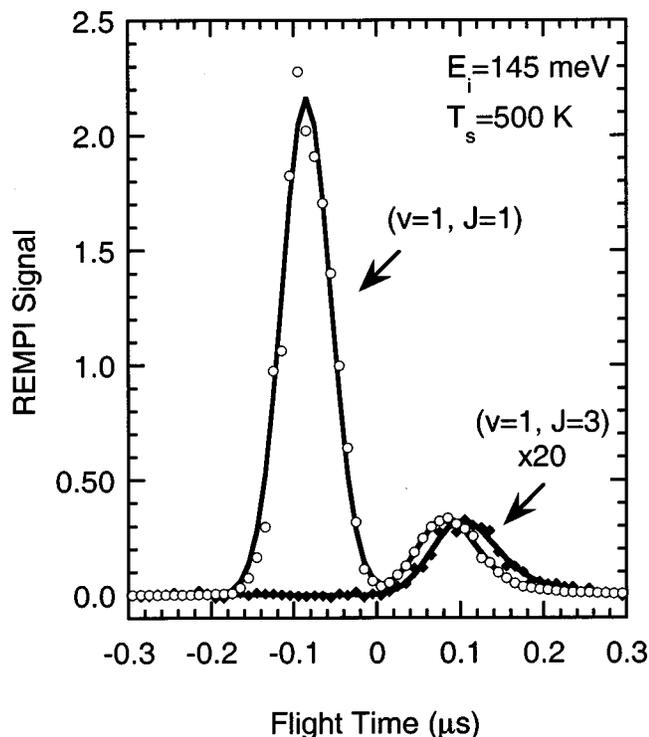
FIG. 1. Time-of-flight spectra of H_2 in the $v=1$ state scattered from Cu(100). The incident $(v=1,J=1)$ pulse reaches the surface at time zero. Molecules leaving the surface appear in the spectrum at positive times. Note: The signal for $(v=1,J=3)$ has been multiplied by 20.

FIG. 2. Time-of-flight spectra of H_2 in various states scattered from Cu(100), showing vibrational relaxation. The incident $(v=1,J=1)$ pulse, shown as a solid line, is a fit to the data like that shown in Fig. 1 for this energy. Molecules leaving the surface appear in the spectrum at positive times.

served simply by scanning the probe laser to the correct wavelength.

III. RESULTS AND DISCUSSION

Typical time-of-flight spectra for H_2 incident on and scattered from Cu(100) are shown in Figs. 1, 2, and 7. Plotted is the REMPI signal as a function of time. The time zero is set after the measurement to be the time that the peak of the incident pulse reaches the surface, so that signal at negative time corresponds to molecules approaching the surface, and signal at positive time to molecules leaving the surface. Time zero is determined by following the incident and scattered signals as the probe focus is translated along the direction of the molecular beam. As the focus is moved toward the surface the incident and scattered signals move closer in time. A plot of the peak TOF position versus focal position is a straight line: The slope is the velocity and the intercept is the position of the surface.

Figure 1 shows TOF data for molecules in the pumped state and molecules that have undergone rotational excitation within $v=1$. The data in Fig. 2 again shows the pumped state, and also shows molecules that have undergone vibrational relaxation and rotational excitation. For clarity, the fit (described below) for the pumped state signal is shown in Fig. 2. Note in particular the relative scale factors for the signals on different transitions relative to the $v=1,J=1$ signal: All the inelastic transitions observed are much weaker than the elastically scattered state.
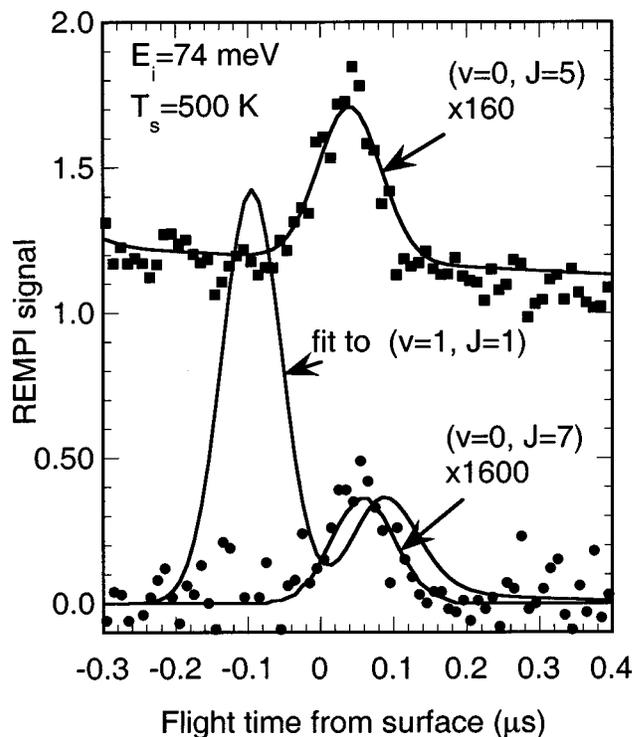
The offset apparent for the $v=0,J=5$ final state data shown in Fig. 2 is real and results from the thermal background of $J=5$ molecules present in the parent molecular beam pulse. This pulse is roughly 10 μs in duration by the time it reaches the surface. On the time scale of the pump–probe measurement (typically 1 μs), it then appears nearly flat. This thermal background for $J=3$ is about 25 times larger than for $J=5$, and about 160 times larger for $J=1$. These signal strengths are such that efforts to observe relaxation into final states $v=0,J=3$ and $v=0,J=1$ were unsuccessful.

In order to determine absolute probabilities for scattering into the different final states we need to integrate both the incident and scattered signals over time and space. The first step in the process is to integrate the TOF spectra. However, a density to flux correction must first be applied since the detection probability is velocity dependent:[24] Slower moving molecules have a higher probability of being ionized since they spend longer in the probe laser focal volume. We convert the observed TOF spectra into a flux weighted basis by fitting each spectrum to a model that uses (a) a flowing Maxwellian velocity distribution and (b) a reasonable functional form for the assumed angular distribution, typically $\cos^n \theta$ where n is a fitting parameter. Once the fit is completed the corresponding flux-weighted distribution is calculated and used in subsequent analysis. The correction ranges from 1% to 20%, larger for slow product channels such as $(v=1,J=3)$, and smaller for the other channels. Next, the scattered flux must be integrated spatially. With the probe laser beam very close to the surface, and the effective focal volume
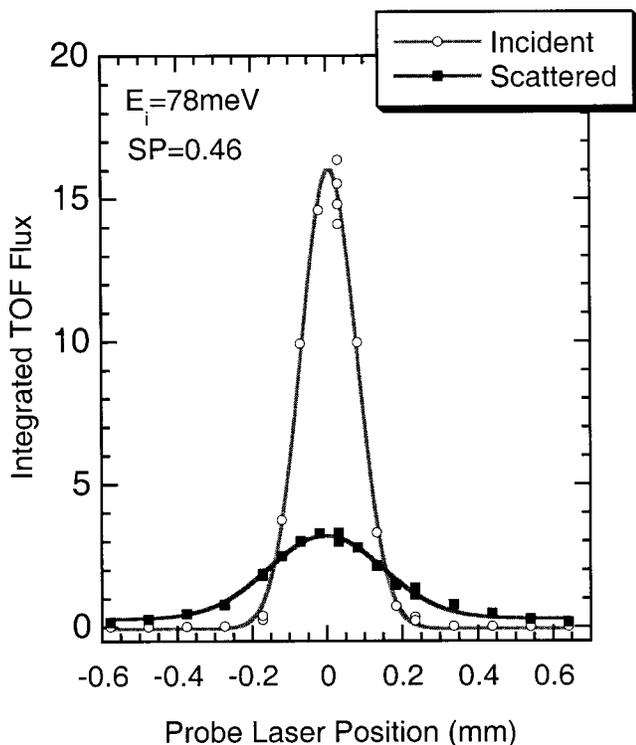
FIG. 3. Spatial profiles of the incident and scattered flux of $H_2(v=1,J=1)$ for clean Cu(100) at an incident energy of 78 meV and a surface temperature of 500 K. Each point represents the integral over time of TOF curves of the type shown in Fig. 1.

FIG. 4. Survival probability of $H_2(v=1,J=1)$ scattered from Cu(100) at 500 K as a function of incident translational energy.

longer than the width of the molecular beam, the probing process effectively integrates over the coordinate along the laser propagation direction. We estimate the angular acceptance for out-of-plane scattering (that is along the laser propagation direction) to be ± 80 degrees. Finally we translate the probe laser beam in steps along the last coordinate, perpendicular to both the laser propagation direction and the molecular beam direction. At each position, a TOF spectra is acquired, converted to flux weighting, and integrated.

We break further analysis of the observed scattering distributions into three parts: survival or elastic scattering in $v=1,J=1$; rotationally inelastic scattering into $v=1,J=3$; and vibrational relaxation into $v=0,J=5$, and $v=0,J=7$.

A. Elastic scattering

An example of the spatial integration results is shown in Fig. 3 for the elastic scattering in the $(v=1,J=1)$ state. Each data point in the figure is the integral over flight time at a fixed vertical position of the probe laser. The figure shows that the spatial distribution of the scattered molecules is broader than for the incident one. Each data set (incident and scattered) is fit to a Gaussian function, and the area of the fit is taken to be the relative, integrated flux. The ratio of the scattered area to the incident area is the survival probability, and for the data shown in Fig. 3 is 0.46 ± 0.05.

We have measured the survival probability for the $(v=1,J=1)$ state as a function of incident translational energy. The results are shown in Fig. 4. We find a gradual decrease in survival probability from 0.81 to 0.30 over a range of translational energies from 31 to 180 meV. This is in contrast
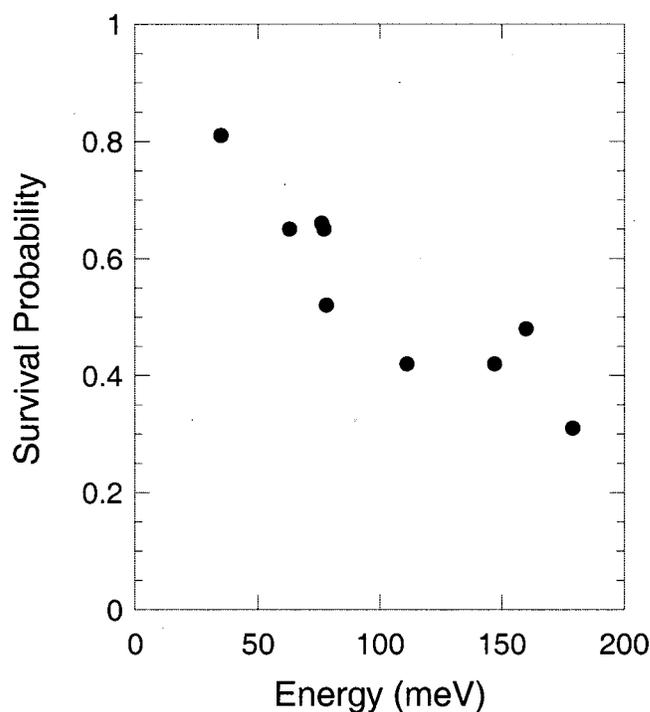
to the results of Hodgson and co-workers[16] for H_2–Cu(111), who reported an abrupt decrease in the survival for the $(v=1,J=0)$ state: they fit their data to a tanh function and obtained a decrease in survival from maximum to zero over a range of incident energy of less than 100 meV.

We have reported results similar to those shown here for the survival probability in the H_2–Cu(110) system although that set of measurements was not as complete as the one reported here.[18] In our previous work the full spatial integration was done at only one incident energy, E_i, and the shape of the spatial distribution was assumed to be the same for other E_i. Here we have directly measured the spatial profile at each translational energy.

One possible explanation for the decrease in survival probability is that a dissociative adsorption channel is opening up. To pursue this idea, we compare our loss measurements with results from state-resolved associative desorption experiments of Rettner, Michelsen and Auerbach for H_2 on Cu(111),[1] no such experiments having been reported for Cu(100). Rettner et al. found their measurements were consistent with s-shaped absorption functions of the form $S_0 = \Lambda[1+\text{erf}(x)]/2$ where $x=(E_n-E_0)/W$, E_n is the energy associated with motion normal to the surface, E_0 is the energy at which half the maximum (Λ) is reached, and W is a width parameter. For the $v=1$ state they determined $\Lambda = 0.25$, $W=0.16$ eV, and $E_0=0.3$ eV. Using these values, the dissociative adsorption probability for $H_2(v=1)$ is calculated as 0.002 at 30 meV and 0.05 at 0.2 eV. These values are much too low to account for the decrease seen in our experiment. Although their results are for Cu(111) and our measurements are made using Cu(100), it is unlikely that the difference in crystal faces is responsible for the discrepancy.
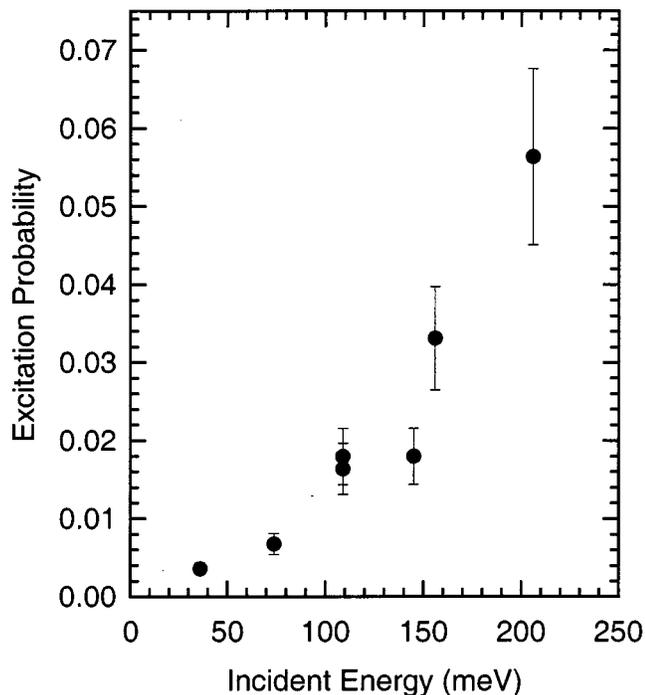
FIG. 5. Inelastic scattering probability for $H_2(v=1,J=1)\rightarrow(v=1,J=3)$ as a function of incident translational energy at a surface temperature of 500 K.

FIG. 6. Final translational energy vs incident translational energy for $H_2(v=1,J=1)\rightarrow(v=1,J=3)$ at a surface temperature of 500 K. The solid line represents expected results for pure translation-to-rotation coupling.

Rendulic et al.[3] measured adsorption probabilities for H_2 on the three low index faces of copper using heated beams, and found a small (roughly 25 meV) shift in the sticking curves between Cu(111) and Cu(100) with sticking being slightly higher on Cu(111) at equivalent energies. In addition, Michelsen and Auerbach fit the results of Rendulic et al. for Cu(100) to a variety of model sticking functions and obtained a threshold of 0.26–0.35 eV and a width of 0.05–0.10 eV, not too different from the results for Cu(111) given above. The conclusion we reach is that the loss shown in Fig. 4 is inconsistent with the sticking functions of Rettner et al., and so is unlikely to be a result of dissociative adsorption. We next consider possible inelastic loss channels.

B. Rotationally inelastic scattering

The TOF data in Fig. 1 also show evidence of rotationally inelastic scattering within the $v=1$ state, specifically excitation from $J=1$ to $J=3$. Two things are readily apparent from the data: (1) The amount of inelastic scattering is weak, compared to the elastic scattering; and (2) the rotationally excited molecules are moving more slowly that the elastically scattered ones, indicating a translational-to-rotational coupling. The small excitation probability is in qualitative agreement with results of Hodgson et al.,[16] who were unable to observe any transfer (within their signal to noise ratio) from $J=1$ to 3 scattered from Cu(111) at energies up to 200 meV.

We found the probability of rotational excitation to depend on both the incident translational energy and on the surface temperature. The dependence on translational energy is shown in Fig. 5. The probability increases to roughly 5% at the highest energy at which we made measurements, 205 meV. Also worth noting is the fact that no obvious threshold
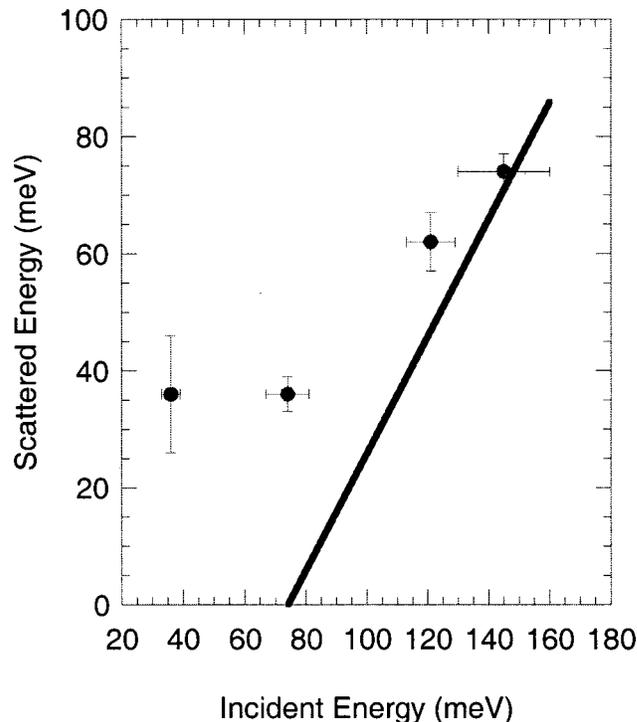
is seen. We can qualitatively compare our results for excitation from $J=1$ to 3 to the results of Hodgson et al.[16] for $J=0$ to 2 for scattering off Cu(111). They found a rapid increase in excitation probability above threshold followed by a leveling off. This plateau occurred above about 150 meV, or roughly three times the $J=0$ to 2 level spacing. We did not find the $J=1$ to 3 excitation probability to level off, however our maximum incident energy was 205 meV or somewhat less than three times the $J=1$ to 3 energy gap. Note that Hodgson et al. plotted the ratio of scattered signals ($I_{J=2,\text{ scattered}}/I_{J=0,\text{ scattered}}$), so that both an increase in rotational excitation and a decrease in survival would lead to an increase in this ratio. We report signals ratioed to the incident flux, and so we measure each of these factors separately.

Figure 5 shows that rotational excitation is seen for incident translational energies that are less the energy gap between the $J=1$ and 3 levels ($\Delta E=74$ meV). In this case, some part of the excitation energy is coming from the surface. We have measured the final translational energy for the rotational excitation channel for several incident energies. The results are shown in Fig. 6 for a surface temperature of 500 K. Shown for reference on this figure is a solid line representing pure translation-to-rotation energy transfer. The vertical difference between the data point and the line is the net amount of energy contributed by the surface. As the incident translational energy is raised, the process becomes more nearly internally elastic, with less energy taken from the surface.

The rotational excitation also depends on surface temperature. TOF spectra showing this dependence are shown in Fig. 7 for an incident energy of 79 meV and surface tem-
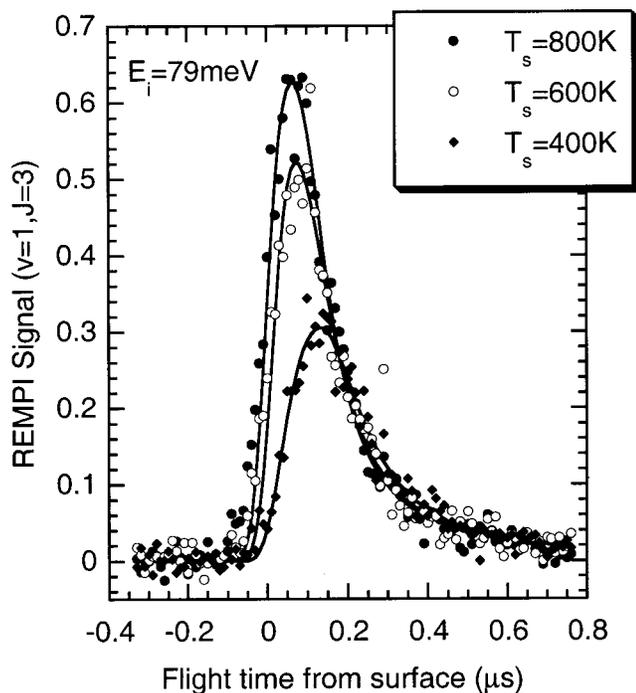
FIG. 7. Time-of-flight curves for vibrationally elastic, rotationally inelastic scattering for different surface temperatures at an incident energy of 79 meV.

peratures from 400 to 800 K. Note that as the surface temperature is increased, not only does the excitation probability increase, but the peak of the TOF curve shifts to earlier times. The excitation uses whatever energy source is available: At low-surface temperature more energy must come from translation, at high-surface temperature more energy comes from the surface, and less from translation.

The surface temperature dependence was analyzed as in our previous studies of H_2 scattering from palladium,[12,13] by plotting the excitation probability logarithmically versus the reciprocal of T_s, that is in an Arrhenius form. The results of this analysis are shown in Fig. 8. Also shown for comparison is the surface temperature dependence for $J=1$ to 3 rotational excitation within the ground vibrational state, measured in a separate, one-laser experiment done at the same incident beam energy. The slope of the lines through the data give the apparent activation energy. For the $v=0$ data, this slope is 74 meV, which is exactly the $J=1$ to 3 energy gap. For the $v=1$ data, the slope is only 45 meV, considerably smaller than the energy gap.

We observed a similar phenomena for rotational excitation of $H_2(v=0)$ scattered from palladium, and discussed it in terms of the motion of the molecule on the elbow potential commonly plotted for dissociation of diatomic molecules on surfaces.[12,13] The picture is that the molecule gets part way round the corner of the elbow before scattering off the surface. The rotational excitation occurs near the turning point in this trajectory where the molecular bond is stretched. This stretching increases the moment of inertia, which decreases the rotational constant, and compresses the rotational energy levels and level spacings. We propose a similar interpretation here, and suggest that the vibrationally excited molecules are

high enough in energy to explore the region of the PES near the barrier to reaction. The molecules in the ground vibrational state do not probe very far around the corner, so the bond is not stretched at all and the apparent activation energy is just the level spacing. This concept of surface–molecule forces acting on a molecule with an extended bond has been discussed by Miura et al.[10] in model calculations for H_2–Cu(111) and also by Wang et al.,[11] although neither group considered surface temperature effects. Miura et al. show that the increase in excitation probability with increasing incident energy is faster for H_2 in $v=1$ that in $v=0$. They explain this in terms of decreased vibrational energy for $v=1$ molecules near the surface (because of the weakened H–H bond since they sample the PES near the barrier), with the vibrational energy that is freed up available for rotational excitation.

C. Vibrationally inelastic scattering

The data plotted in Fig. 2 show vibrational relaxation accompanied by rotational excitation for two final states in $v=0, J=5$ and 7. These are the two highest J-states that are lower in total energy than the $v=1, J=1$ state pumped in the incident beam. The $v=0, J=9$ state would represent a substantial net excitation, and we did not observe it. As noted earlier, the background for the $J=5$ state seen in Fig. 2 is real and results from thermal population in this state present in the parent beam pulse. The difference in time scale between the parent pulse and the packet of molecules produced
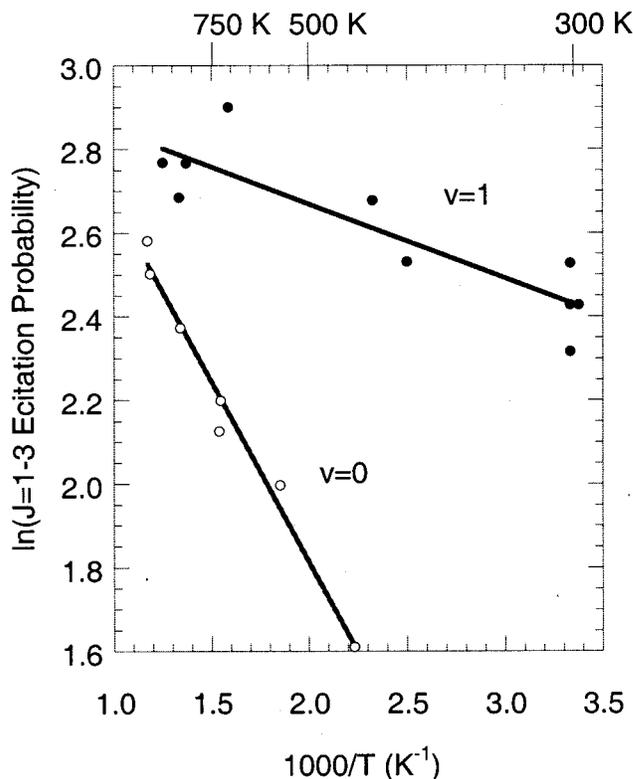

FIG. 8. Arrhenius plots of ($J=1 \rightarrow 3$) rotational excitation vs inverse surface temperature for molecules in $v=0$ (open symbols) and $v=1$ (solid symbols) at an incident energy of 74 meV.

TABLE I. Probability of vibrational relaxation of $H_2(v=1, J=1)$ into ($v=0, J=5$) and ($v=0, J=7$). $T_s = 500$ K.

Surface	E_i (meV)	($v=0, J=5$)	($v=0, J=7$)
Cu(100)	74	0.009	0.0005
Cu(100)	36	0.02	...
Cu(110)	78	0.016[a]	0.002[a]

[a]Note: These values do not take the spatial distribution of the scattered signal into account.

by stimulated Raman excitation allows us to temporally separate and identify those molecules associated with relaxation from the incident $v=1$ flux even in the presence of a substantial $v=0$ background. However, the thermal background in the $J=3$ and 1 states of $v=0$ are much larger than that in $J=5$, and precludes observation of relaxation into these states with the current signal-to-noise ratio of our experiment.

Several aspects of the TOF data of Fig. 2 are readily apparent: (1) the relaxation channels are very weak, with the ($v=0, J=7$) state more than three orders of magnitude smaller than the elastically scattered ($v=1, J=1$); (2) the scattering probability into ($v=0, J=7$) is roughly twenty times less than into ($v=0, J=5$) even though the ($v=0, J=7$) state is closer in total rovibrational energy to the ($v=1, J=1$) initial state; (3) the signals associated with vibrational relaxation appear earlier in time than the elastically scattered flux, indicating that at least some of the energy freed up in vibrational relaxation is appearing in the translational degree-of-freedom.

The vibrational relaxation probabilities are listed in Table I for the two final states of $v=0$ observed for scattering from both Cu(100) and Cu(110). Complete spatial profiles were not measured for these two final states because of the low signal levels. Instead we have assumed that the profiles had the same shape as those measured for scattering within $v=1$, and the measured signal at normal reflection was scaled accordingly. The results are similar for the two surfaces with the relaxation probability being somewhat higher on the more open Cu(110) plane. Also shown in Table I is a result for an incident energy of 36 meV for relaxation into ($v=0, J=5$). This is intended to show that the relaxation does not change a great deal at lower energy and we do not think the difference between the 36 and 74 meV result is significant. The ($v=0, J=7$) channel was too weak to be measured at the lower energy.

The final translational energies for molecules scattered into ($v=0, J=5$) and ($v=0, J=7$) were measured at an in-

cident energy of 78 meV and a surface temperature of 500 K. Table II shows a summary of all the energy exchange for these final channels. Also presented in this Table are corresponding measurements from a Cu(110) sample, showing very similar results. Inspection of the data in Table II shows that within a factor of 2 to 3, all degrees-of-freedom participate in the scattering with energies of 100–500 meV being lost or gained. The final $v=0$ state rotational and translational energies are anti-correlated, that is the energy released in vibrational relaxation is shared between rotation and translation. This is fully consistent with microscopic reversibility and the finding by Rettner et al.[15] that vibrational excitation comes at the expense of translation, and that the vibrationally excited state has lower average rotational energy. However, by summing up all the energy transfer within the molecule (shown in the last column of Table II), we find that for the $v=0, J=5$ channel a comparable amount of energy is missing and must have been lost to surface degrees-of-freedom. This is similar to our previous results for the vibrational relaxation of H_2 on Pd(111), and the amounts of energy lost are quite similar for the same final states.

D. Flux balance

The amount of inelastic scattering observed does not come close to accounting for the loss out of the pumped state. The missing flux must be in one of two channels: either in the two final J-states of $v=0$ that we cannot measure ($J=1$ and 3), or dissociated on the surface. (Note: No relaxation was ever observed into even rotational states, consistent with a negligible ortho-para conversion probability in direct scattering.) Both of these alternatives present difficulties when compared with previous work.

First, as discussed above, based on analysis of state resolved measurements of H_2 produced by recombinative desorption, the dissociative adsorption probability for $H_2(v=1, J=1)$ at our translational energies should be too small to account for the loss we find. One factor that might account for this discrepancy is the following: in the desorption experiments, surface H is supplied by permeation out of the bulk. Atoms in the bulk have an elevated potential with respect to surface atoms. If the atoms recombine on the surface rapidly with respect to the time needed for equilibration, some of the excess energy may appear in the product molecule, perhaps as translational energy. This process is analogous to a hot atom reaction (or Eley–Rideal) reaction in which the hot atom comes out of the bulk and not out of the gas phase.[25] Thus, analysis of premeation-desorption data

TABLE II. Summary of energy gains and losses in the vibrational relaxation of H_2 from Cu(100) and Cu(110). Vibrational relaxation releases 516 meV. E_i and E_s are the incident and scattered translational energies, ΔE_T is the change in translational energy, ΔE_R the change in rotational energy, and ΔE_{total} is the total energy lost by the molecule. All energies are listed in meV.

Final state	E_i	E_s	ΔE_T	ΔE_R	ΔE_{total}
Cu(100) ($v=0, J=5$)	74±7	285±35	211	207	98±36
Cu(100) ($v=0, J=7$)	74±7	151±23	77	400	39±24
Cu(110) ($v=0, J=5$)	78±7	251±33	173	207	136±34
Cu(110) ($v=0, J=7$)	78±7	176±10	98	400	18±12

could overestimate the energy needed for dissociative adsorption (in which the atoms do not go directly into the bulk). Essentially, this is saying that dissociative adsorption and desorption following permeation may not be microscopically reverse processes.

To check for evidence of dissociation, we attempted to observe a buildup of adsorbed hydrogen on the surface by looking for an increase with time of the reflectivity of the $v=1, J=1$ state as the surface becomes possibly covered with dissociated H_2 at low temperature. In our previous work on palladium, this was straightforward to do because the unpumped H_2 was readily absorbed by the surface, and the buildup of a layer of adsorbed H took only a few minutes. In the present case on copper, the unpumped H_2 ($v=0$) has a very low adsorption probability and only the ($v=1$) molecules potentially adsorb. Based on our estimate of the beam flux, the Raman pumping efficiency, and the volume illuminated by the pump lasers, we estimate that we should produce coverage of roughly one monolayer of dissociated $H_2(v=1, J=1)$ in about three hours. This time is comparable to the amount of time where we begin to see changes in surface cleanliness as a result of adsorption of background gases. Our measurements along these lines were inconclusive and remain a subject for future study, perhaps involving more sensitive surface science probes of adsorbed hydrogen. Note that the estimated coverage is in a small area of roughly 0.1 by 4.5 mm, and attempts to measure any adsorbed hydrogen by standard thermal desorption were also unsuccessful.

The second possibility to account for the loss from the ($v=1, J=1$) state is that relaxation is occurring into the ($v=0, J=1$) and ($v=0, J=3$) states. Both calculations and measurements of vibrational excitation in the H_2–copper system indicate that rotational relaxation tends to accompany the increase in vibration, with part of the excitation energy coming out of rotation. Microscopic reversibility suggests that vibrational relaxation should be accompanied by rotational excitation. Furthermore, calculations for relaxation of $H_2(v=1, J=0)$ on Cu(100)[5] show most of the relaxation is accompanied by rotational excitation with the $J=4$ state being the most populated. Additional calculations have been carried out for $H_2(v=1, J=1)$ on the same surface and will be presented elsewhere, along with comparison to this experiment,[14] but the same general trend as found in Ref. 5 is found: The probability for scattering into final J-states of 1, 3, and 5 are equal within a factor of 2. Since at $E_i=74$ meV we find a survival probability of roughly 0.60 and a total relaxation into ($v=0, J=5$) and ($v=0, J=7$) of less than 0.02, this line of reasoning implies that the all missing flux in our experiment is unlikely to be present in the $J=1$ and 3 states. One factor is missing from the calculations and that is the presence of surface degrees-of-freedom. Our results show that the surface absorbs some part of the energy released in the relaxation, particularly for the ($v=0, J=5$) final state; it may be that energy dissipation into the surface is more important for the ($v=0, J=1$) and ($v=0, J=3$) channels and enhances relaxation into these states. At the present time, we think this is the most likely explanation. Future improvements to the experiment may allow us to observe these states, or at least to place meaningful upper limits to the relaxation probabilities.

IV. CONCLUSION

We have measured elastic and inelastic scattering of H_2 prepared in the ($v=1, J=1$) state from a Cu(100) surface for incident H_2 translational energies of 35 to 200 meV, and surface temperatures of 400–800 K. We find a gradual decrease in the survival probability with incident energy for the initially prepared state from 0.81 at $E_i=35$ meV to 0.30 at $E_i=180$ meV. We find that the probability for inelastic scattering to other rotational and vibrational states is relatively small. The probability for rotational excitation increases with both incident energy and surface temperature. The surface temperature dependence is well described by an Arrhenius analysis; the apparent activation energy for the $J=1-3$ transition is less the energy gap between these two states for gas phase H_2. We interpret this as evidence that the excitation occurs near the surface where the H–H bond is stretched because of the reactive nature of the PES. Vibrational relaxation was observed for two final states ($v=0, J=5$) and ($v=0, J=7$). The sum of all elastic and inelastic scattering probabilities was substantially less than 1. This indicates either a large probability for relaxation into the two rotational states of ($v=0, J=1$) and ($v=0, J=3$) which could not be observed in our experiment because of the thermal population in these states, or significant dissociation of the $v=1$ state. A dissociation channel of this magnitude is inconsistent with probabilities determined from energy- and state-resolved desorption experiments.

[1] C. T. Rettner, H. A. Michelsen, and D. J. Auerbach, J. Chem. Phys. **102**, 4625 (1995).
[2] G. J. Kroes, Prog. Surf. Sci. **60**, 1 (1999).
[3] K. D. Rendulic, G. Anger, and A. Winkler, Surf. Sci. **208**, 404 (1989).
[4] B. Hammer, M. Scheffler, K. W. Jacobsen, and J. Norskov, Phys. Rev. Lett. **73**, 1400 (1994).
[5] G. J. Kroes, E. J. Baerends, and R. C. Mowrey, J. Chem. Phys. **107**, 3309 (1997).
[6] G. R. Darling and S. Holloway, Rep. Prog. Phys. **58**, 1595 (1995).
[7] G. Wiesenekker, G. J. Kroes, and E. J. Baerends, J. Chem. Phys. **104**, 7344 (1996).
[8] A. Gross, S. Wilke, and M. Scheffler, Surf. Sci. **357-358**, 614 (1996).
[9] W. Dong and J. Hafner, Phys. Rev. B **56**, 15396 (1997).
[10] Y. Miura, H. Kasai, W. A. Dino, and A. Okiji, Surf. Sci. **438**, 254 (1999).
[11] Z. S. Wang, G. R. Darling, and S. Holloway, Surf. Sci. **458**, 63 (2000).
[12] M. Gostein and G. O. Sitz, J. Chem. Phys. **106**, 7378 (1997).
[13] E. Watts and G. O. Sitz, J. Chem. Phys. **111**, 9791 (1999).
[14] E. Watts *et al.*, J. Chem. Phys. **114**, 495 (2001).
[15] H. A. Michelsen, C. T. Rettner, D. J. Auerbach, and R. N. Zare, J. Chem. Phys. **98**, 8294 (1993).
[16] A. Hodgson, P. Samson, A. Wight, and C. Cottrell, Phys. Rev. Lett. **78**, 963 (1997).
[17] M. Gostein, H. Parikhteh, and G. O. Sitz, Phys. Rev. Lett. **75**, 342 (1995).
[18] M. Gostein and G. O. Sitz, J. Vac. Sci. Technol. A **14**, 1562 (1996).

J. Chem. Phys., Vol. 114, No. 9, 1 March 2001

Scattering of H$_2$($v=1,J=1$) from Cu(100)   4179

[19] M. Gostein, E. Watts, and G. O. Sitz, Phys. Rev. Lett. **79**, 2891 (1997).

[20] D. A. McCormack *et al.*, Phys. Rev. Lett. **82**, 1410 (1999).

[21] H. A. Michelsen, C. T. Rettner, and D. J. Auerbach, in *Surface Reactions*, edited by R. J. Madix (Springer-Verlag, Berlin Heidelberg, 1994), Chap. 6.

[22] H. A. Michelsen and D. J. Auerbach, J. Chem. Phys. **94**, 7502 (1991).

[23] E. E. Marinero, C. T. Rettner, and R. N. Zare, Phys. Rev. Lett. **48**, 1323 (1982).

[24] M. Gostein and G. O. Sitz, in *Laser Techniques for State-Selected and State-to-State Chemistry III*, edited by J. W. Hepburn (SPIE, Bellingham, WA, 1995).

[25] C. Rettner and D. Auerbach, Phys. Rev. Lett. **74**, 4551 (1995).